Defence Science Journal, Vol. 75, No. 2, March 2025, pp. 149-158, DOI : 10.14429/dsj.20144

Multidisciplinary Wing Layout Optimisation

Hakan Demir[#,*] and Necmettin Kaya[$]

[#]Graduate School of Natural and Applied Sciences, Bursa Uludağ University, Bursa - 160 59, Turkey
[$]Department of Mechanical Engineering, Bursa Uludağ University, Bursa - 160 59, Turkey
[*]E-mail: hakandemir@uludag.edu.tr

ABSTRACT

Studies to enhance the static and dynamic characteristics of aircraft often lead to increased weight, resulting in higher power demand and fuel consumption, which can reduce flight time. This study formulates two optimisation problems aimed at improving the wing's static and dynamic properties without adding weight. The optimisation focused on the positioning of the wing's spar and rib structures, with static and dynamic properties defined as objective functions. The first objective was to reduce wing displacement and increase its first natural frequency, while the second aimed to raise the ratio of the wing's first torsional frequency to its first bending frequency to enhance flutter speed. A parametric wing model was created, and analyses were performed in ANSYS, automated with a Python script. A surrogate model was built using Modified Latin Hypercube Sampling (MLHS), and optimization was conducted using multi-objective genetic algorithms and genetic algorithms. After optimization, the wing's natural frequency increased by 4 %, displacement decreased by 5.7 %, and the torsional-to-bending frequency ratio improved by 6.61 %.

Keywords: Wing design; Multidisciplinary optimisation; Flutter; Layout optimisation

NOMENCLATURE

C	: Chord length of the airfoil
$f1$	: First bending natural frequency
FEA	: Finite element analysis
SM	: Surrogate model
MDO	: Multidisciplinary optimisation
CFD	: Computational fluid dynamics
GPR	: Gaussian process regression
RMSE	: Root mean square error
MLHS	: Modified latin hypercube sampling
LHS	: Latin hypercube sampling
Ma	: Mach number
P_{cr}	: Critical buckling coefficient
Δ_{max}	: Maximum deformation
LHS	: Latin hypercube sampling
$f4$	: First torsional natural frequency
GBDM	: Gradient based deterministic method
ANN	: Artificial neural networks

1. INTRODUCTION

One of the most important components of an aircraft is the wing, which carries the fuel tanks and a significant part of the load during various situations such as take-off, climb, cruise, descent, and landing. The essential structural parts of an aircraft wing are spars and ribs. The spar structure is one of the primary components of the wing. It extends from the wing root to the wing tip and connects the wing to the aircraft fuselage. The spars can be perpendicular to the vetter line or at a certain angle. The number of spars in some wings can vary depending on the aircraft. Spars are crucial for transferring aerodynamic loads, particularly the lift force, from the wing to the fuselage, where primary structural joints are established. Additionally, spars are critical in resisting bending and torsional moments induced by aerodynamic forces, thus maintaining the wing's structural integrity.

The rib structures, which impart the external shape to the wing, serve to prevent distortion of the wing's shape due to aerodynamic loads while simultaneously resisting torsional moments in conjunction with the spar[1]. A schematic representation of the aircraft wing is shown in Fig. 1.

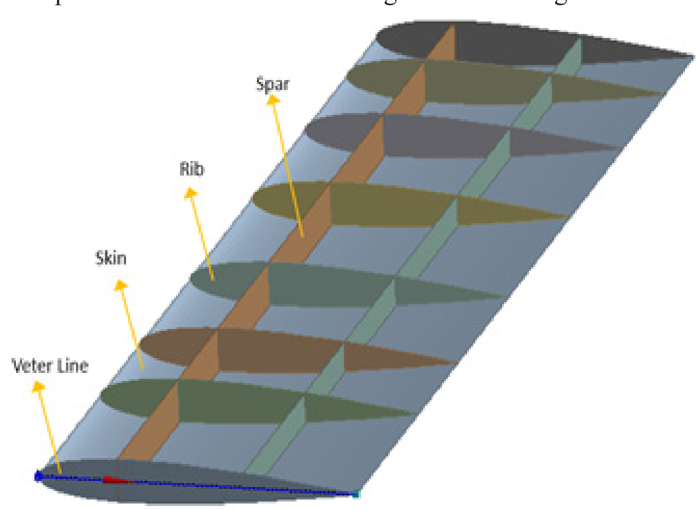

Figure 1. Schematic representation of aircraft wing.

Received : 16 May 2024, Revised : 08 October 2024
Accepted : 22 November 2024, Online published : 24 March 2025

During flight, an aircraft wing is subjected to various forces, including drag, lift, weight, and engine thrust. Lift is generated by the pressure difference between the wing's upper and lower surfaces, with higher pressure beneath the wing. However, the wing has a limited capacity to withstand these forces and may suffer structural damage if subjected to excessive loads. For instance, in a rapid descent or sudden maneuver, reduced air pressure above the wing and increased pressure below can cause significant bending, potentially leading to structural failure. Therefore, wings must be designed to endure these bending loads effectively[2]. In addition to static loads, wings are also exposed to dynamic loads during flight. Vibrations from aerodynamic effects and engine operation can resonate with the wing's natural frequency, causing excessive stress and potential damage. Modal analysis is used to determine dynamic properties such as natural frequencies and mode shapes, focusing on torsional and bending modes. Pranjal[3], *et al.* investigated materials to minimise wing vibration and concluded that aluminium is the most suitable.

Flutter is one of the most critical dynamic structural issues an aircraft wing can encounter. This situation arises from the interaction of aerodynamic, elastic, and inertial forces, leading to dynamic instability. Literature indicates that the flutter speed depends on the first bending and torsional frequencies, as well as their ratio. Tola[4], *et al.* demonstrated that increasing this ratio can enhance the flutter speed of a structure. Tola[4], *et al.* revealed that the flutter speed of a structure can be increased by enhancing the torsional frequency and the bending frequency ratio, as this process increases the stiffness.

Numerous optimisation studies have been conducted to improve aircraft wing performance. Guo[5] demonstrated that replacing a metal wing box with a composite one could reduce weight by up to 40 %. Similarly, Son[6], *et al.* showed a 22.9 % increase in the first natural frequency with only a 3.4 % increase in mass by optimising the spar section. Yu Li[7], *et al.* emphasised the importance of spar positioning in enhancing wing stiffness, noting that improper placement can reduce resistance to torsion and bending. Falco[8], *et al.* optimised the thickness and position of wing spars and ribs, increasing the critical load capacity while reducing weight. Aung[9] achieved an 18.17 % weight reduction in UAV wing spars through layer optimization based on maximum deformation criteria. Khadse[10], *et al.* performed modal analyses on a wing with a NACA 64A215 airfoil, finding close agreement between theoretical and Ansys simulation results. Rechtik[11], *et al.* optimised thicknesses of 2D skin and spar structures for objectives like empty weight and L/D ratio, while Farzan[12], *et al.* focused on weight reduction under buckling and compliance constraints using composite skins and ribs.

In flutter speed optimization, Melike[13], *et al.* increased the flutter speed of the AGARD 445.6 wing by 17 % through adjustments in taper ratio, sweep angle, elasticity, and shear modulus. Asadi[14], *et al.* explored curvilinear fibre paths to maximize flutter speed, and Akshayraj[15], *et al.* used Ansys-Multifield Solver to analyse the impact of wing thickness and span changes, predicting up to 5 % variation in flutter speed. In predictive modeling, Yuce[16], *et al.* compared Random Forest Regression and ANN for estimating crack growth life in a fighter aircraft wing joint, highlighting the benefits of machine learning for accuracy and efficiency. Jebakumar[17], *et al.* introduced the ALSR-FP algorithm for preventing low-speed departure in high-performance fighter aircraft. Surrogate models are increasingly used to address the high computational demands of traditional optimization methods. Zhang[18], *et al.* applied quadratic polynomial regression, Kriging, and ANN's in an aero-structural optimisation study demonstrating the effectiveness of surrogate-based Multidisciplinary Design Optimisation (MDO) while cautioning against potential errors from ignoring aeroelastic effects. Rasmussen[19], *et al.* proposed a two-step optimisation approach for a joined-wing aircraft, using polynomial regression-based surrogate modeling for design exploration. Paiva[20], *et al.* compared surrogate models for predicting aerodynamic coefficients, concluding that Kriging and neural networks are more effective than polynomial regression for complex scenarios.

The first study considers two objective functions: minimising displacement and maximising the first natural frequency. Displacement is prioritized due to its significant impact on wing structural stability, flight safety, and aerodynamic performance. Excessive displacement can lead to induced wave drag and reduce passenger comfort in commercial aircraft. Thus, wing deflection is a critical parameter. The first natural frequency, representing the wing's resistance to mechanical vibrations, is crucial for structural integrity and flight safety. A low first natural frequency may result in unwanted vibrations and deformation under aerodynamic loads, especially at high speeds and in turbulent conditions. Maintaining an appropriate first natural frequency enhances aerodynamic performance and flight stability, making it a key factor in wing design. This study aims to address a gap in the existing literature by performing a multi-objective optimisation of rib and spar positions. The objective is to enhance the static and dynamic properties of the structure without increasing the weight, while also improving flutter speed by optimising the torsional-to-bending frequency ratio.

While previous studies have focused on improving static and dynamic properties by altering wing geometry, material properties, and composite characteristics, this study employs a surrogate model to achieve these goals without increasing mass. Additionally, unlike traditional approaches that focus solely on ribs or assume equal rib spacing, this study offers a comprehensive optimisation of both rib and spar structures, providing a more sophisticated solution to enhance wing performance.

2. METHODOLOGY

In this optimisation study, a parametric wing model was created, and fluid, static, and dynamic analyses were performed using Ansys software. The entire process was automated through a Python script. A modified Latin Hypercube Sampling (LHS) method was employed to generate an experimental dataset, which was then processed by a Python script used to create the necessary geometry and conduct the analyses. This resulted in the development of a surrogate optimisation model.

A Design of Experiment (DoE) table was constructed using MATLAB's lhsdesign function, which generated a Latin hypercube sample matrix to ensure even distribution across each factor's range. This table served as the foundation for building the surrogate model. Automatic analyses were performed using the data from the DoE table, producing the necessary data for the surrogate model. The optimisation process was then conducted using this surrogate model, resulting in significant time and computational cost savings. Since the optimisation algorithm relies on the surrogate model to obtain results, it eliminates the need for real-time analyses during each iteration, thus avoiding the necessity of conducting real analyses at every step. Figure 2 illustrates the flow diagram of the wing design optimisation process. In this study, pressure is considered only in a unidirectional Fluid-Structure Interaction (FSI) scenario, affecting the initial structural analysis but not the subsequent optimization steps.

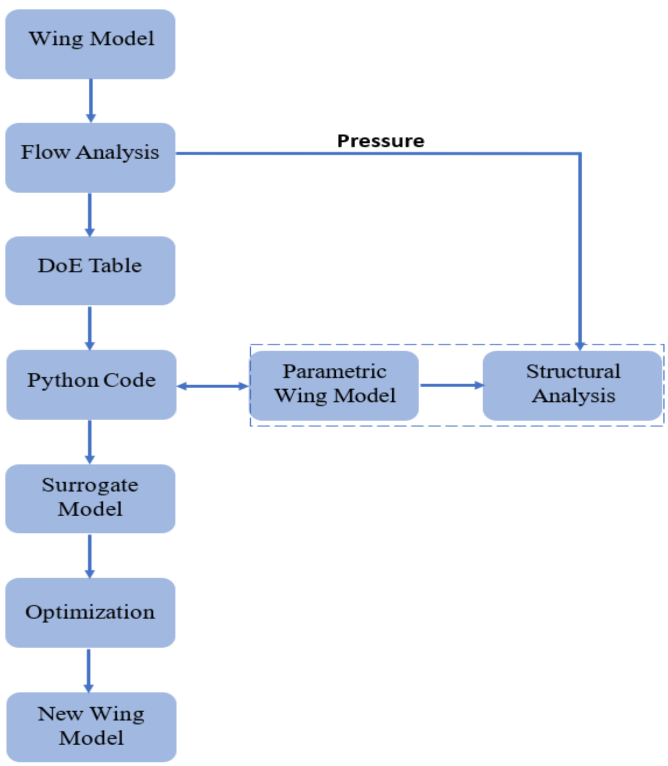

Figure 2. Flow diagram of wing design optimisation.

2.1 Wing Model

The wing model used in this study features a NACA 0012 airfoil with a rectangular planform, having a root and tip chord length of 0.8 meters and a span of 3 meters. The simplified aircraft wing model, which includes two stringers and eight ribs, is illustrated in Fig. 3(a). In this model, the spar, ribs, and skin structures all have a thickness of 5 mm and are constructed from aluminium alloy. The positions of the spar and ribs within the wing model are employed as design variables, as shown in Fig. 3(b). The model is represented using the Shell281 element, selected for its efficiency in processing time and computational cost and its suitability for accurately capturing the characteristics of the wing components. The material properties of the wing model include a Young's modulus of 71000 MPa, a density of 2770 kg/m³, and a Poisson's ratio of 0.33.

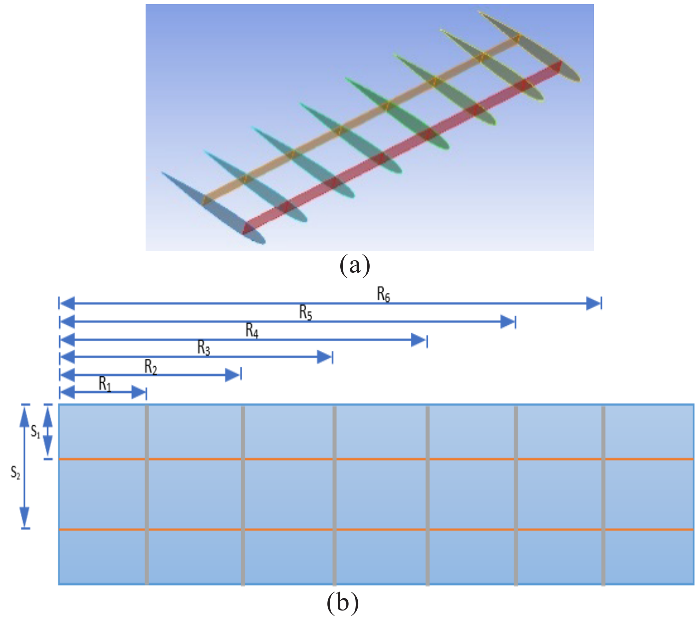

Figure 3. (a) Wing model; and (b) Wing spar and rib design variables.

In this study, R1 represents the distance of the first rib from the wing root, with R2 through R6 symbolizing the distances of the second to sixth ribs from the wing root, respectively. The objective is to find the optimal positions for these ribs based on defined objective functions, ensuring that there is no blind spot in the wing space. To achieve this, both dynamic and normal variable ranges are used, as shown in Table 1, to scan the entire wing area thoroughly. The variable ranges designed as dynamic range and normal range are given in Table 1.

Table 1. Dynamic ranges of design variables

Variable	Dynamic range	Normal range
R_1	150 mm<R_1<1500mm	200 mm<R_1<600 mm
R_2	(R1+100) mm<R2<1800 mm	650 mm<R_2<1050 mm
R_3	(R2+100) mm<R3<2100 mm	1100 mm<R_3<1500 mm
R_4	(R3+100) mm<R4<2400 mm	1550 mm<R_4<1950 mm
R_5	(R4+100) mm<R5<2700 mm	2000 mm<R_5<2400 mm
R_6	(R5+100) mm<R6<2900 mm	2450 mm<R_6<2850 mm
S_1	0.2 C<S1<0.75C	0.2C<S_1<0.5C
S_2	(S1+0.15) C<0.9C	0.6C<S_2<0.9C

In normal range optimisation, the design variables are constrained by predefined static limits, confining the design space to specific boundaries established before the optimization process begins. This approach may overlook potential optimal solutions. Conversely, dynamic range optimisation offers greater flexibility by allowing the variable ranges to be dynamically adjusted based on the values of preceding design parameters. This adaptive approach helps avoid blind spots within the design space, ensuring a more comprehensive exploration and potentially uncovering superior solutions. As can be seen in Table 1, the lower and upper limits of each variable in the dynamic range change based on the value taken by the previous variable. As illustrated by the following example, defining the dynamic range offers a number of advantages: Suppose R1 has a value of 450. If in a dynamic range definition, R2 is defined in the range (500, 1800), while in a normal range definition, R2 is defined in the range (650, 1050), and R2 takes a value of 850, then in the dynamic range definition, R3 can be defined in the range (900, 2100). In contrast, in the normal range definition, R3 is defined within the range (1100, 1500). This shows that variables defined within a dynamic range, with wider upper and lower limits, have the potential to give better results by covering a wider parameter space. Dynamic range optimisation offers significant advantages by exploring a broader design space. In defining the ranges for design parameters, care was taken to prevent aeroelastic issues, such as static torsional separation, by maintaining a specified distance between the ribs and spars.

2.2 Computational Fluid Dynamics (CFD) Model

The aerodynamic loads acting on the wing were computed using the commercial finite volume solver ANSYS Fluent software. The wing model was placed within a C-type computational domain. To ensure accurate results in numerical simulations, proper discretisation of the computational domain is crucial. A substantial amount of time is dedicated to mesh generation to achieve mesh independence in the results[21]. As shown in Fig. 4, the mesh structure created was designed with a higher cell density, using smaller elements in regions close to the wing geometry.

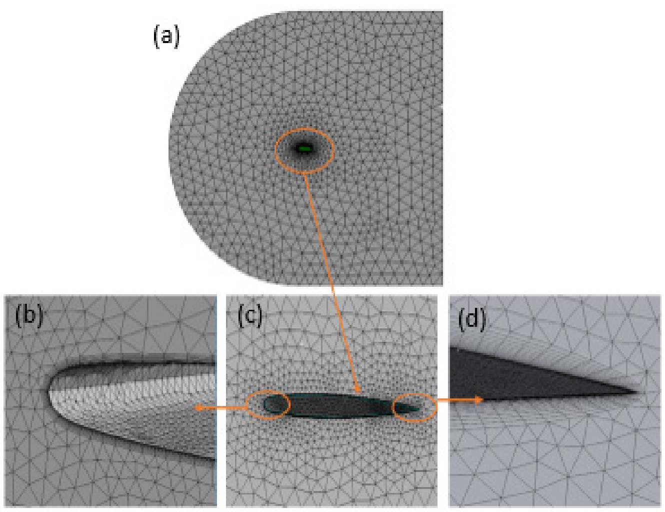

Figure 4. Mesh structure around the wing: (a) mesh around the wing; (b) leading edge; (c) wing detail; and (d) trailing edge.

Table 2. Mesh independency study

Number of cells	Lift coefficient	Drag coefficient
2500000	0.586	0.0203
3000000	0.597	0.0186
3500000	0.616	0.0175
4000000	0.622	0.0168
4500000	0.624	0.0165
5000000	0.625	0.0163

2.2.1 Mesh Independence

A thorough mesh independence study was conducted to verify the adequacy of the final mesh. Table 2 shows the lift and drag coefficients with a Reynolds number of 10^6 and angles of attack of 6°.

2.2.2 Validation

The 3D analysis of the vortex type yielded more realistic results compared to the 2D operation NACA0012 airfoil. However, despite conducting a 3D analysis in this study, it is crucial to verify the reliability of the findings against existing literature[22]. To verify the calculations for conformity with the literature, the calculations were performed under the conditions of $Re=10^6$.

The computational results of lift coefficients were compared with the experimental data from Ladson[23]*, et al.* and Gregory[24]. The comparison revealed a maximum margin of error of 5 % between the calculated values and the literature. This close agreement indicates that the numerical procedure and the Spalart-Allmaras turbulence model employed for the simulations exhibited acceptable accuracy.

In this study, the Spalart-Allmaras turbulence model was utilised, and simulations were performed using ANSYS Fluent. This model was chosen for its suitability in aerodynamic simulations, particularly for flows around wings and airfoils. The validation against experimental results confirms that both the turbulence model and the numerical procedure in Fluent were appropriate and accurate for the study's objectives.

2.2.3 Boundary Conditions

The boundary conditions were set at high speed with a Mach number of 0.6, a temperature of 288.15 K, and a pressure of 101.325 Pa. When performing flow analyses in structures such as wings and rockets, the Spalart-Allmaras turbulence model is known to provide more accurate results in shorter time. Hence, the Spalart-Allmaras turbulence model was used in this study.

2.4 Design of Experiment Study

Surrogate models, used in the optimisation process, are approximate models that replace the finite element model. Optimisation solution algorithms are inherently iterative, and demand repeated solving of the finite element model.

When the dataset used to construct a surrogate model is randomly generated based on the variables, the resulting surrogate model may lack the predictive capability to represent all aspects of the system. In such scenarios, employing systematic sampling methods is essential. In constructing any surrogate model, the primary objective is to minimise the error in the model's predictions for specific inputs. The selection of the dataset used to construct the surrogate model significantly influences the achievement of this goal. Latin Hypercube Sampling stands out as a preferred method when exploring sampling techniques, as it selects non-overlapping design points and effectively fills points on the surface, thus enhancing the quality of the surrogate model. The dataset obtained by Latin Hypercube Sampling (LHS) was used to construct the surrogate model, and improvements were made to enhance its predictive capabilities. In optimisation methodologies, the primary aim is to minimise or maximise the objective function. Consequently, the surrogate model offers more precise predictions for points in proximity to the minimum or maximum values, thereby yielding more accurate results in optimisation problems. Hence, within this study, a novel method dubbed MLHS was devised through modifications to the LHS technique. MLHS exhibits superior predictive capabilities compared to LHS, particularly in regions neighbouring the minimum or maximum values of the objective functions.

In Modified Latin Hypercube (MLHS) sampling, the process begins with performing LHS sampling using half the predetermined number of samples. Subsequently, H design points are selected from the sampling points closest to the maximum or minimum value of the function based on the conducted experiments. Following the selection of these design points, the lower and upper intervals of the variables are expanded to D %. Then, experimental sampling using LHS is carried out for each of the H design points individually, employing half of the previously determined number of MLHS samples.

The Goldstein-Price test function given in Eqn. 1 is used to evaluate whether MLHS can give superior results compared to LHS with the same number of experiments.

$$f(x)=\left[\left(x_1+x_2+1\right)^2\left(19-14x+3x^2-14y+6xy+3y^2\right)\right]$$

$$\left[30+\left(2x+3y\right)^2\left(18-32x+12x^2+48y-36xy+27y^2\right)\right] \quad (1)$$

The Goldstein function is a global optimisation test function. As seen in Eqn. 1, it has two variables. The global minimum point is $x* = (0, -1)$, and $f(x) = 3$. The graph of the Goldstein-Price test function is shown in Fig. 6. In order to compare the MLHS with the LHS method, the following procedure was followed: for the first model, 100 samples were generated using the LHS model. For the second model, 50 samples were generated using LHS. Following this, five design points close to the minimum value of the function were selected from the 50 samples. The lower and upper values of each design point were then expanded by 20 %, and ten samples were generated for these five design points separately using LHS. The MLHS method is shown in Fig. 5.

In Fig. 6, the first part shows the 100 data sets generated with LHS; the second part shows the LHS sampling, which is the first stage of MLHS; the design points shown with red dots in this part symbolise the five design points closest to the minimum of the test function.

The last part of Fig. 6 shows that the lower and upper values of the selected 5 (H) design points are expanded by 20 % (D) and combined with the second figure in Fig. 13 with 5 * 10=50 different LHS samples, giving a total of 100 design points. The DoE table obtained with MLHS is shown in Fig. 13, section 3, while the DoE sample table obtained with LHS is shown in Fig. 6.

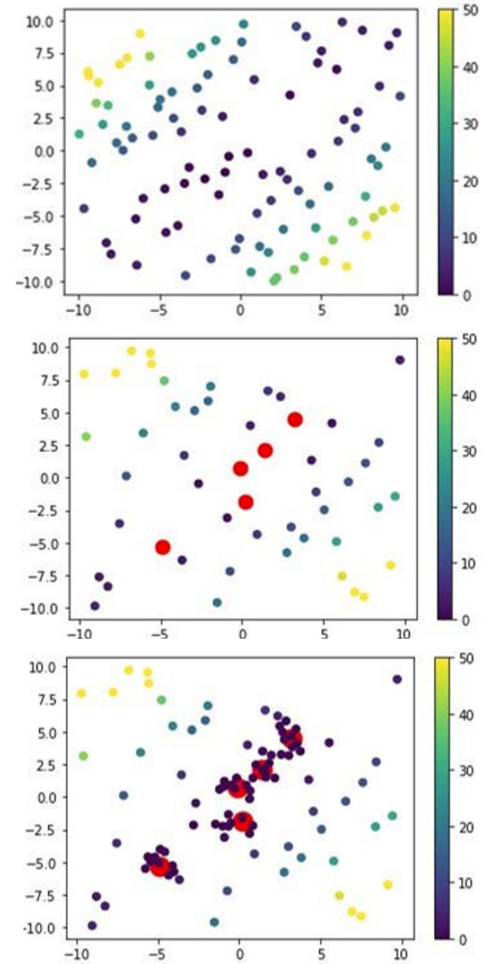

Figure 5. Graph of the Goldstein-Price test function and Graphical representation of the dataset obtained using LHS and MLHS.

To compare the MLHS and LHS models, two surrogate models were created using MLHS and LHS data with artificial neural networks using the sample data shown in Fig. 6. MLHS and LHS were compared using three randomly selected test points, and the results are shown in Table 3. As can be seen in Table 3, the surrogate model constructed using MLHS had a better predictive ability. In addition, the surrogate model generated by the MLHS method clearly shows better predictive ability than the other model, especially as it approaches the values that minimise the function.

As shown in Table 3, the MLHS method is able to make better predictions.

Table 3. Comparison of LHS and MLHS

Method	Test Point 1 (x1=0.52, x2=0.95)	Test Point 2 (x1=2.35, x2=-0.25)	Test Point 3 (x1=0.265, x2=-0.84)
Function	6678	17518	18.9
LHS	6747	16897	26.08
MLHS	6596	17775	19.19

2.5 Surrogate Modeling

The MLHS method was used to build a surrogate model for optimisation, and a DoE table with 200 samples was created. In the first study, two output variables (first natural frequency and displacement) and eight input variables (R1, R2, R3, R4, R4, R5, R6, S1, S2) were used to build the surrogate model.

There are many methods in the literature for building surrogate models, but it is necessary to test which methods are most appropriate for our data in the DoE table. The methods in Matlab were used,, and their predictive ability was tested using R-squared. The model with the least error based on the R-squared values, and deemed most suitable for our dataset, is the neural network model. The R-squared value for the neural network model is calculated to be 0.95. These results indicate that the model fits the data very well and has a high ability to explain the data.

2.6 Optimisation

The optimisation study carried out as part of this study was carried out using the Matlab optimisation module and the surrogate model created with the neural network.

The Matlab optimisation module has two multiobjective optimisation algorithms, paretosearch and gamultiobj, and three optimisation algorithms, fmincon, ga, and pattern search.

In the first study, a multiobjective position optimisation of the wing spar and rib elements was performed to minimise the displacement value and maximise the first natural frequency value.

The objective functions are given in Eqn. 2.

$$\min\left(\Delta_{\max}\right), \max\left(f_1\right) \tag{2}$$

Δ_{max} represents the maximum deformation of the wing, and f_1 represents the first natural frequency of the wing. The optimisation constraint of the wing's total weight is given in Eqn. 3.

$$g_1 = m_{wing0} - m_{wing} \geq 0 \tag{3}$$

m_{wing} and m_{wing0} are the wing's total weight and the wing's initial weight, respectively.

In this study, the dynamic range was used to create DoE table patterns to determine the position variable ranges of the spar and rib structures.

The second study carried out in this study was a multiobjective position optimisation of the wing spar and rib elements to maximise the frequency ratio as our objective function in this study, based on the study [3], which shows that the wing flutter speed is directly proportional to the ratio of the first torsional frequency to the first bending frequency.

The objective functions are given in Eqn. 4.

$$\max\left(f_4 / f_1\right) \tag{4}$$

f_4 represents the first torsional natural frequency of the wing, and f_1 represents the first bending natural frequency of the wing.

The weight constraints, which are the optimisation constraint, are given in Eqn. 5.

$$g_1 = m_{wing0} - m_{wing} \geq 0 \tag{5}$$

m_{wing} and m_{wing0} are the wing's total weight and the wing's initial weight, respectively.

The optimisation variables and their ranges are the same as those in the first study.

The wing model of the three optimal results selected from the Pareto optimal set as a result of the first study and the optimal result obtained in the second study were re-analysed to check for both buckling and stress, and while no buckling was observed, the stress value was well below the yield value of the material.

3. RESULTS AND DISCUSSION

The parametric modelling of the wing model, the determination of the pressure load acting on the wing, and the static and dynamic analysis were carried out in the Ansys Workbench environment. The analysis processes were automated using script code written in Python.

The data set was generated using a modified Latin Hypercube sampling method. A regression learner toolbox was used in Matlab to create a surrogate model, which was then validated and used in the optimisation process. In order to decide on the optimisation algorithm to be used in the multiobjective optimisation study carried out as part of the first study, the Paretosearch and Gamultiobj algorithms were tested in Matlab, and it was decided to use the Gamultiobj algorithm as it gave more appropriate results. To compare the wing models derived from optimisation, a reference wing was generated, and a comparative analysis was conducted. In the reference wing model, the ribs are evenly distributed from the root to the tip of the wing, while the spars are positioned between 20 % and 70 % of the wing chord, adhering to common practices in the literature. The distribution of ribs and spars in the reference wing model is illustrated in Fig. 6.

Table 4 provides the variable values of the three optimal results selected from the set of Pareto-optimal solutions, as well as the reference wing model used for comparing the optimisation results. Table 5 displays the comparison between the results obtained from the three optimal solutions selected from the Pareto-optimal solution set and the values derived from the FEA model. As can be seen in Table 5, the values of the three optimal results are close to the FEA results. Table 6 provides information on how three optimal solutions selected from the Pareto optimal solution set improved over the reference result.

In multiobjective optimisation studies, users have the flexibility to select the result set based on the desired objective function from the set of Pareto-optimal solutions obtained through Pareto search methods. For instance, referring to Table 6, if displacement is a critical factor, Optimal Result-2 can be chosen. Similarly, if the first natural frequency holds more significance, Optimal Result-3 can be preferred. Alternatively, if both factors are equally important, Optimal Result-1 may be selected.

The representation of the position distribution of the wing spar and rib structures for the reference result and the Optimal Result-1, Optimal Result-2, and Optimal Result-3 solution set is shown in Fig. 6.

In multiobjective optimisation problems, the obtained Pareto optimal set allows the end user to select the desired design point according to his preferences, thus providing

Table 4. Pareto solution set

Design Point	Variables							
	R_1	R_2	R_3	R_4	R_5	R_6	S_1	S_2
Optimal result-1	0.3	0.62	1.02	1.45	1.95	2.5	0.295C	0.595C
Optimal result-2	0.28	0.55	1.1	1.4	2.08	2.47	0.275C	0.69C
Optimal result-3	0.32	0.65	0.85	1.27	1.75	1.95	0.27C	0.70C
Reference wing	0.428	0.856	1.28	1.71	2.14	2.568	0.20C	0.70C

Table 5. Comparison of FEA and surrogate model solution

	Displacement surrogate model	Displacement FEA	First natural frequency surrogate	First natural frequency FEA
Optimal result-1	12.06	12.25	10.93	10.98
Optimal result-2	11.96	12.09	10.88	10.96
Optimal result-3	12.18	12.35	10.97	10.79
Reference result	12.92	12.68	10.55	10.73

Table 6. Comparison of Pareto solution set reference result

	Displacement	Per cent improvement displacement	First natural frequency	Per cent improvement first natural frequency
Optimal result-1	12.06	6.66	10.93	3.78
Optimal result-2	11.96	7.28	10.88	2.94
Optimal result-3	12.18	5.73	10.98	4.07
Reference result	12.92	-	10.55	-

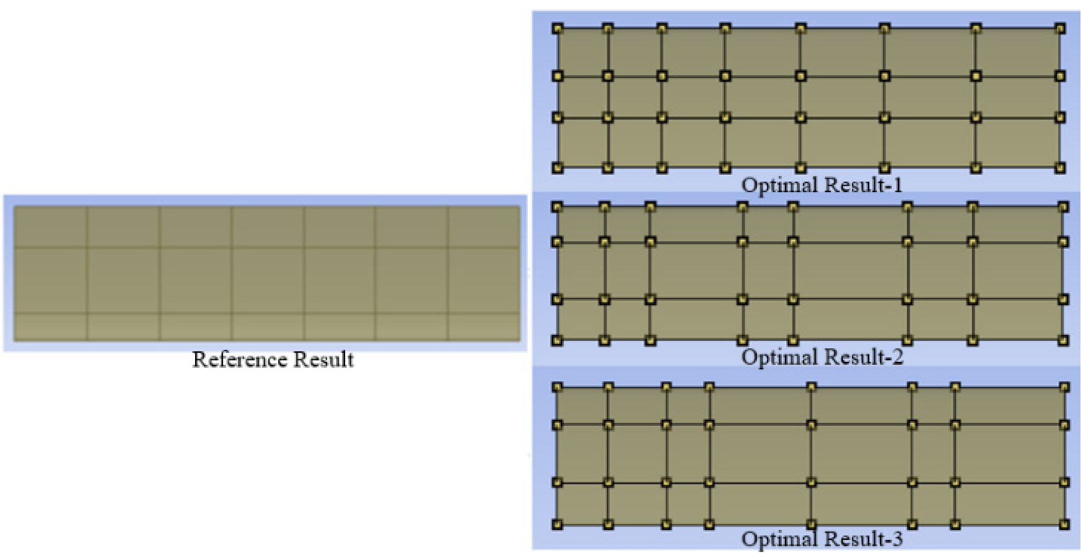

Figure 6. Reference result and Optimal Result-1,2,3 solution wing layout.

flexibility. As shown in Table 4, when the results of the selected optimal solutions from the Pareto-optimal set are compared with the reference values, an improvement in both static and dynamic characteristics is achieved without an increase in mass. As shown in Fig. 6, to enhance the static and dynamic characteristics of the wing spar and rib structures, the ribs are positioned closer to the center of the vetter line and in proximity to each other. Figure 6 illustrates three different placements of the ribs. The increase in distances between the ribs from the wing root to the tip is attributed to the distribution of aerodynamic forces. Typically, aerodynamic forces exerted on the wing surface are higher at the wing root due to its connection to the fuselage, where larger loads are transferred. Thus, it is crucial to provide greater resistance at the root by incorporating more ribs. Consequently, the configuration presented in Optimal Result-1 aligns with both established knowledge and literature. In Optimal Result-2, the spars are spaced further apart compared to Optimal Result-1, while the

Table 7. Pareto solution set

	Variables							
Design point	**R_1**	**R_2**	**R_3**	**R_4**	**R_5**	**R_6**	**S_1**	**S_2**
Optimal result	0.38	0.77	1.3	1.72	2.23	2.62	0.28C	0.65C
Reference result	0.428	0.856	1.284	1.712	2.14	2.568	0.25C	0.70C

Table 8. Comparison of optimal solution with the reference result

	Ratio of torsional frequency to bending frequency	**Per cent improvement result**
Optimal result	7.03	5.41
Reference result	6.65	-

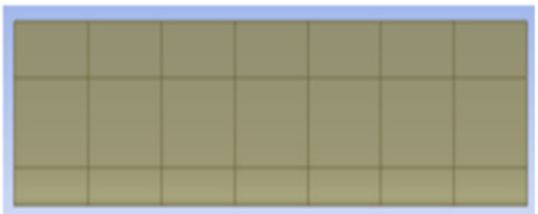

Reference Result

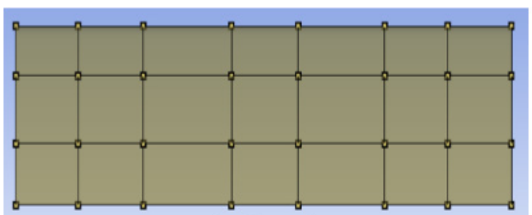

Optimal Result

Figure 7. Reference result and Optimal Result solution wing layout.

ribs are positioned close to the wing tip in pairs. Similarly, in Optimal Result-3, the spars resemble those in Optimal Result-2, whereas the ribs are positioned near the wing tip in groups of one and two. This arrangement of ribs and spars enhances the static and dynamic properties of the wing without increasing its mass.

The optimal result obtained as a result of the optimisation study conducted using the genetic algorithm method (ga) in the Matlab program in the second study is given in Table 7 & Table 8.

The extent to which the optimal solution obtained as a result of optimisation increases the ratio of torsional frequency to the bending frequency of the reference wing is shown in Table 7 & Table 8..

The position distribution of the wing and nerve structures of the reference result and the optimal result are shown in Fig. 7.

As can be seen in Fig. 7, the wing spars and ribs are positioned for maximum flutter speed, with the spars close to the leading edge of the wing and close together and the ribs in pairs close together. This arrangement of ribs and spars improves the flutter speed of the wing without increasing its mass.

The wing model of the three optimal results selected from the Pareto optimal set as a result of the first study and the optimal result obtained in the second study were re-analysed to check for both buckling and stress, and while no buckling was observed, the stress value was well below the yield value of the material.

4. CONCLUSION

In this study, two optimisation problems were defined to improve the static and dynamic properties of the wing without increasing the weight of the wing by optimising the positions of the main structural parts of the wing, namely the spar and rib structures. A multiobjective and multidisciplinary study was carried out using the surrogate method, and the following results were obtained:

- As a result of the first study, the wing displacement improved by 6.66 %, and at the same time, the first natural frequency of the wing increased by 3.78 %. The non-resonant safety margin was therefore increased.
- As a result of the second study, the ratio of the wing's first torsional frequency to its first bending frequency improved by 6.61 %.
- As can be seen in both studies, we can improve the desired property for the wing by optimising the wing spar and rib structures according to a systematic, rather than random, placement.
- Instead of using the finite element method to obtain the required objective and constraint functions for optimisation, the surrogate model method was used, which resulted in efficient utilisation of both time and computational resources.
- In this study, the predictive ability of the surrogate model is improved using the MLHS method developed for experimental sampling.
- Furthermore, the results of the optimisation in both studies show that if we did not use the dynamic range definition, the positions of the wing spars and ribs obtained as a result of the optimisation would not be like this. Therefore, it is concluded that better results can be found when the wing positions as a dynamic range scan a wider area.
- This study shows that the position of the wing rib and spar positions has a significant effect on many structural and dynamic properties of the wing, such as stiffness, flutter speed, and natural frequency.
- Due to the wing structure, the dimensions of the spar structures change as their positions change, which can lead to an increase in wing weight. In the first study, there was an increase in wing weight of approximately 0.6 % due to the spar, while in the second study, the decrease was 0.1 %.
- In future work, optimising the placement of components such as beam bulkheads and longerons can improve the desired properties of the fuselage.

REFERENCES

1. Sohaib, M. Parameterized automated generic model for aircraft wing structural design and mesh generation for finite element analysis. Linkoping's University, Sweden, 2011. (MSc Thesis).
2. Dogan, C. Design optimization of composite I-beam wing spars with the corrugated web. Doğuş University, Istanbul, 2014. (MSc Thesis).
3. Agrawal, P.; Dhatrak, P.; & Choudhary, P. Comparative study on vibration characteristics of aircraft wings using finite element method. *Mater. Today Proc.*, 2021, **46**(1), 176–183. doi: 10.1016/j.matpr.2020.07.229.
4. Ceyhun, T. & Melike, N. Investigation of the effect of thickness, taper ratio and aspect ratio on fin flutter velocity of a model rocket using response surface method. *In* 7th International Conference on Recent Advances in Space Technologies (RAST), Istanbul, Turkey, 2015, pp. 27–32.
5. Guo, S. Aeroelastic optimization of an aerobatic aircraft wing structure. *Aerosp. Sci. Technol.*, 2007, **11**(5), 396–404. doi: 10.1016/j.ast.2007.01.003.
6. Lovely, S. The effect of wing spar cross-sectional profile variation on the Unmanned Aerial Vehicle (UAV) natural frequency. *In* IOP Conf. Ser.: Mater. Sci. Eng., 2021, **1062**, 012032. doi:10.1088/1757-899X/1062/1/012032.
7. Yu, L.; Jingwu, H.; & Yuexi, X. Layout design optimization of spars under multiple load cases of the high-aspect-ratio wing. World Academy of Science, Engineering and Technology, 2017, 10007949. doi: 10.5281/zenodo.113225.
8. Falco, S.A. & Faria, A.R. Optimization of a simple aircraft wing. 23rd International Council of the Aeronautical Sciences Congress (ICAS 2001-01), 2002, 8–13 September, Toronto, Canada. Stockholm: CAS.
9. Aung, N.L.; Tatarnikov, O.; & Aung, P.W. Optimization of composite wing spars for an unmanned aerial vehicle. *J. Sci. IOP Conf. Ser.: Mater. Sci. Eng.*, 2020, **971**(5), 52–76. doi:10.1088/1757-899X/971/5/052076.
10. Khadse, N.A. & Zaweri, S.R. Modal analysis of aircraft wing using ANSYS workbench software package. *Int. J. Eng. Res. & Technol. (IJERT)*, 2015, **4**(7). doi: 10.17577/IJERTV4IS070291.
11. Rechtik, S. & Daoud, F. Structural wing optimisation targeting economical mission performance of a passenger aircraft. *The Aeronaut. J.*, 2023, **127**(1316), 1717–1736. doi:10.1017/aer.2023.21.
12. Nasab, F.F.; Geijselaers, H.J.M.; Baran, I.; Akkerman, R.; & de Boer, A. Optimization of the interacting stiffened skins and ribs made of composite materials. *AIAA J.*, 2020, **58**(4), 1836–1850. doi:10.2514/1.J058415.
13. Melike, N. & Pınar, A. Flutter based aeroelastic optimization of an aircraft wing with analytical approach. *In* Structural Dynamics and Materials Conference, 2012. doi:10.2514/6.2012-1796.
14. Asadi, D.; Farsadi, T.; & Kayran, A. Flutter optimization of a wing–engine system with passive and active control approaches. *AIAA J.*, 2021, **59**(4), 1422–1440.
15. Akshayraj, N. & Sriram, A.T. Effect of wing geometric parameters on flutter speed. *Int. J. Vehicle Struct. & Syst.*, 2022, **14**(1), 121–127. doi:10.4273/ijvss.14.1.25.
16. Yüce, Z.; Yayla, P.; & Taşkın, A. A comparative investigation of random forest regression and artificial neural networks for predicting crack growth life of a fighter aircraft wing joint under spectrum loading. *Def. Sci. J.*, 2023, **74**(01), 119–126. doi: 10.14429/dsj.74.18954.
17. Jebakumar, S.; Pashilkar, A.; & Sundararajan, N. A novel design approach for low speed recovery of high performance fighter aircraft. *Def. Sci. J.*, 2022, **72**(4), 505–515. doi:10.14429/dsj.72.17821.
18. Zhang, K.-S.; Han, Z.-H.; Li, W.-J.; & Song, W.-P. Coupled aerodynamic/structural optimization of a subsonic transport wing using a surrogate model. *J. Aircraft*, 2008, **45**(6), 2167–2171. doi: 10.2514/1.35709.
19. Rasmussen, C.C.; Canfield, R.A.; & Blair, M. Optimization process for configuration of flexible joined wing. *Struct. Multidisc. Optim.*, 2008, **37**(3), 265–273. doi: 10.1007/s00158-008-0230-6.
20. Paiva, R.M.; Carvalho, A.R.D.; Crawford, C.; & Suleman, A. Comparison of surrogate models in a multidisciplinary optimization framework for wing design. *AIAA J.*, 2010, **48**(5), 995–1006. doi: 10.2514/1.J050092.
21. Bashir, M.; Zonzini, N.; Longtin Martel, S.; Botez, M.; Ceruti, A.; & Wong, T. Numerical investigation of the dynamic stall reduction on the UAS-S45 airfoil using the optimised airfoil method. *The Aeronaut. J.*, 2024, **128**(1321), 441–468. doi: 10.1017/aer.2023.62.
22. Çakıroğlu, R.; Tanürün, H.E.; Acır, A.; Üçgül, F.; & Olkun, S. Optimization of NACA 4412 augmented with a gurney flap by using grey relational analysis. *J. Braz. Soc. Mech. Sci. Eng.*, 2023, **45**(3), 1–18. doi:10.1007/s40430-023-04089-x.
23. Ladson, C.L. Effects of independent variation of mach and reynolds numbers on the low-speed aerodynamic characteristics of the NACA 0012 airfoil section. NASA TM 4074, October 1988.

ACKNOWLEDGEMENTS

Within the scope of TUBITAK 2244 Industrial Doctorate Program, we would like to acknowledge the scholarship support (Project No: 118C100).

CONTRIBUTORS

Mr Hakan Demir obtained his BSc degree in Mechanical Engineering at Uludag University in 2019. His research areas are aided design, interdisciplinary studies, optimisation, and aerospace engineering.

In the current study: Problem conceptualisation, solver development, validation, and preparation of the manuscript.

Prof Dr Necmettin Kaya obtained his PhD from Uludag University and working as a Professor at the Mechanical Engineering Department of Uludag University. His areas of research include: Feature-based modular fixture design, computer-aided design, finite element method, evolutionary algorithms, structural optimisation and additive manufacturing. Contribution int the current study: Problem conceptualisation, investigation and supervision.